MICROFLUIDIC STIFFNESS-DEPENDENT SEPARATION OF RED BLOOD CELLS FOR EARLY MALARIA DIAGNOSIS AND SURVEILLANCE

A Thesis
Presented to
The Academic Faculty

by

Rebecca Byler

In Partial Fulfillment
of the Requirements for the Degree
Bachelors of Science in the
School of Biomedical Engineering

Georgia Institute of Technology
December 2013

MICROFLUIDIC STIFFNESS-DEPENDENT SEPARATION OF RED BLOOD CELLS FOR EARLY MALARIA DIAGNOSIS AND SURVEILLANCE

Approved by:

Dr. Todd Sulchek, Advisor
School of Mechanical Engineering
Georgia Institute of Technology

Dr. Rudy Gleason
School of Biomedical Engineering
Georgia Institute of Technology

Dr. Edward Botchwey
School of Biomedical Engineering
Georgia Institute of Technology

Date Approved: December 10th, 2013

ACKNOWLEDGMENTS

I would like to especially thank my mother and father for their endless guidance, support, and encouragement. I would not be here without them. I would also like to thank my graduate student advisor Billy Wang (PhD candidate) and principal investigator Dr. Todd Sulchek for invaluable assistance with research design, data collection, and both personal and professional mentorship over the past seven semesters. I would also like to acknowledge support from both the President's Undergraduate Research Award (PURA) and the Petit Scholars Program. Finally, I would like to thank all those suffering from malaria that I met on my travels for sparking my interest in humanitarian engineering and for whom this research is dedicated.

TABLE OF CONTENTS

LIST OF TABLES

LIST OF FIGURES

LIST OF SYMBOLS AND ABBREVIATIONS

RBC	Red Blood Cell
*i*RBC	Malaria Infected Red Blood Cell
POC	Point-of-Care
LSM	Lattice Spring Model
E	Young's Modulus
AFM	Atomic Force Microscopy
GTA	Glutaraldehyde
FMA	Formaldehyde
DIA	Diamide
ACD	Citrate-dextrose solution
DPBS	Dulbecco's Phosphate Buffered Serum
PLL	Poly-L-Lysine

SUMMARY

The characterization of the mechanical properties of cells has many broad applications since cell elasticity can indicate pathological state. Notably, many diseases cause significant changes in mechanical properties; principally, at the onset of a malaria infection, the invading parasites decrease the deformability of Red Blood Cells (RBCs) through a variety of structural and molecular changes. Thus, given the difference in mechanical properties between healthy RBCs and malaria infected RBCs (*i*RBCs), there exists the potential to separate human blood by stiffness via a microfluidic platform in order to develop a more sensitive malaria diagnostic test. We report a statistical difference in cell elasticity between RBCs and chemically stiffened *i*RBCs, which mimic the pathophysiology of malaria infection, through the use of Atomic Force Microscopy. We also demonstrate preliminary stiffness-dependent separation of RBCs and chemically mimicked *i*RBCs via microfluidic technology. The future successful completion of this technique directly aids the long-term objective of this project, which is to develop point-of-care microfluidic technologies for malaria diagnosis and population surveillance that improves on the sensitivity of existing malaria Rapid Diagnostic Tests (RDTs).

CHAPTER 1

INTRODUCTION

With over 3.3 billion people at risk for infection, malaria is one of the world's deadliest infectious diseases, causing more than one million deaths per year[1]. In developing countries, over 95% of these deaths are caused by the lack of proper diagnosis and subsequent improper treatment[1]. Thus, the development of low-resource diagnostic tools for developing countries has emerged as a key focus of public health disease diagnosis and surveillance initiatives[2,3,4,5]. In particular, microfluidic point-of-care (POC) diagnostics can be used to detect and monitor infectious diseases in resource-limited areas because they can be easily used in rural endemic areas and allow for real-time monitoring of disease transmission. Recent development in microfluidic technology has provided more opportunities for low cost, high-throughput, POC medical diagnostic tools[2,3,4,5].

Malaria is a mosquito-borne infectious disease caused by the invasion and multiplication of parasitic *Plasmodium* protozoans within Red Blood Cells (RBCs)[6,7]. RBCs can be considered elastic bodies since they must significantly deform as they pass through capillaries[3]. However, the mechanical properties of RBCs drastically change during malaria infection, which causes increased membrane rigidity and decreased deformation[6,8,9]. In addition to increased stiffness due to the inclusion of the parasite, the infected RBC (*i*RBC) can also be stiffened though the presence of crosslink actin in the cytoskeleton[9]. This variance in cell stiffness is significant at a microscopic scale, ranging from 3-50 times stiffer than healthy RBCs, and can used to differentiate otherwise

identical populations[8,10]. This variance in stiffness occurs since RBC elasticity is affected by both the stage of parasite maturation inside the RBC and by the blood parasitemia[8].

Thus, given the difference in mechanical properties between healthy RBCs and *i*RBCs, there exists the potential to separate human blood through microfluidics in order to better detect malaria. Specifically, this study initially aims to (1) empirically measure the difference in stiffness between RBCs and abnormally stiffened RBCs through the use of Atomic Force Microscopy and (2) mechanically separate RBCs and stiffened RBCs via microfluidic channels. These results will aid in the long-term objective of this project, which is to develop microfluidic technologies for malaria diagnosis that improves on the sensitivity of the existing malaria Rapid Diagnostic Tests (RDTs). If successful, a more sensitive diagnostic device, capable of malaria detection earlier than the current standard, will be developed. By detecting malaria earlier, such as in potentially asymptomatic individuals, enhanced population surveillance will be possible.

Malaria

Malaria is a major cause of human suffering and mortality. In particular, malaria is an infectious disease that threatens approximately 3.3 billion people and causes 1 million deaths annually[3,11,12,13,14]. As shown in **Figure 1**, malaria is endemic in over 106 countries and territories, the majority of which are considered to be developing nations[11,12]. Malaria is endemic in these regions because tropical and subtropical climate conditions, including frequent rainfall and warm temperatures, provide ideal habitats for mosquito larvae that host the malaria parasites[3,6,11,12,13,14].

Malaria is caused by the invasion and multiplication of parasitic protozoans of the genus *Plasmodium* within RBCs[1,6,8,9,11,15]. Specifically, there are five species of

Plasmodium that can infect and be transmitted by humans. Of these, *P. falciparum* and *P. vive* cause the majority of the deaths, while *P. ovule*, *P. malaria*, and *P. Knowles* produce a milder form of malaria that is rarely fatal[6,7,15].

Figure 1. The Global Presence of Malaria[11]. Red indicates an endemic country or territory.

The *Plasmodium* parasites are transmitted via the bite of infected *Anopheles* mosquitos, which inject a motile infective form of the parasite (sporozoites) via their saliva into a human's circulatory system during a blood meal[6,7,11,15]. Once in the blood, the sporozoites travel to the liver for an initial infection phase, during which they mature and reproduce asexually to generate thousands of merozoites. Once the merozoites rupture the hepatocytes, they return to the bloodstream to infect and reproduce in RBCs. In particular, merozoites develop into ring forms (early stage), trophozoites, and schizonts to continue parasitic propagation in the human host, as well as develop into gametocytes, which allow for continued propagation outside of the human host as the

parasite looks for a new vector. Gametocytes are taken up with blood when a fertilized mosquito feeds on an infected human, allowing for the development of sporozoites in the new mosquito's gut[3,6,7,11,15]. A more detailed description of the malaria life cycle can be seen in **Figure 2**.

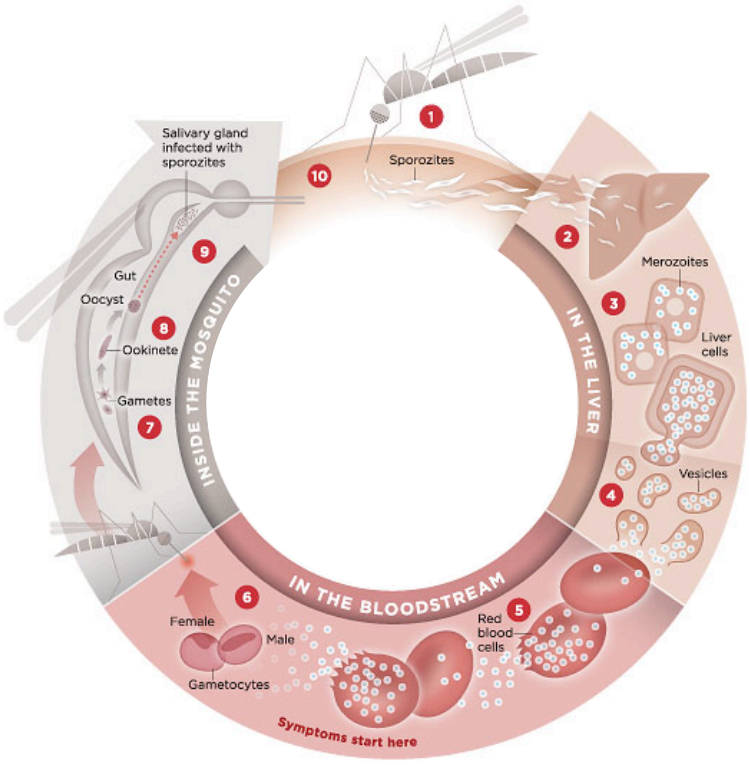

Figure 2. Malaria Life Cycle[23]

Symptoms and Diagnosis

Symptoms of malaria generally emerge 8-25 days following infection[1,2,6,13,15]. As a result, the blood infection phase is also known as the diagnostic phase since most individuals appear asymptomatic during the short liver infection phase[1,2,3,4,5]. Initial manifestations of malaria mimic the flu with symptoms including headache, fever, joint pain, and vomiting; as such, early stage malaria can resemble a number of other common diseases. More advanced malaria can induce symptoms such as paroxysm, or a sudden coldness followed by chills and then recurrent fever, and serious complications including respiratory distress and neurological symptoms (cerebral malaria)[11,12,13,14,15]. Malaria is especially fatal to children, with more than 90% of all fatalities occurring in children[15]. **Figure 3** shows a Ugandan child suffering from malaria. Uganda has the highest

prevalence of malaria compared to other endemic countries with approximately 9.8 million cases annually[11].

Figure 3. Ugandan child suffers from malaria[16]

Given its non-specific clinical symptoms, malaria diagnosis in endemic countries remains difficult[8,13,14]. Currently, malaria is confirmed by microscopy or by antigen-based RDTs (**Figure 4)**[13,14]. Microscopy, or the microscopic examination of blood films for the presence of *Plasmodium* parasites, is the most commonly used method to confirm a malaria infection[11,13]. However, despite its widespread use, correct diagnosis in rural endemic settings is difficult due to the lack of proper facilities and trained technicians to process the results since the accuracy of microscopy is highly correlated with the skill of the person examining the blood films[14]. In fact, it has been shown that the sensitivity of blood films range from 75-90% in optimal settings to 50% in suboptimal settings such as in rural developing countries[8,11,12,13,14]. Although RDTs require little to no training to use, deliver results within an hour, and are often more accurate than microscopy, they are highly variable in diagnostic sensitivity and specificity from company to company[13,14]. Specifically, although RDTs may be more specific than other current diagnostic methods, they are not sensitive enough to detect asymptomatic individuals[1,2,3,4,5]. Increased

Figure 4. Current Malaria Diagnosis Methods including Rapid Diagnostic Tests and Microscopy.

detection sensitivity is needed for early malaria diagnosis and enhanced disease surveillance[12,16]. In fact, current RDTs can only detect 200 parasites/μL, which correlates to a more advanced stage of malaria infection and, in the majority of cases, correlates with a state that can also be diagnosed clinically[17,18,19].

Due to the lack of sensitive point-of-care diagnostic tools and the high costs of current diagnostic tools and a lack of adequate facilities, clinical diagnosis remains the most frequently used method of detection in developing countries despite being imprecise[1,12,13,14,17,18,19]. However, more than 30% of infected individuals will arrive at a medical facility with no fever when seeking treatment[20]. As such, it was reported that over 95% of all malaria cases go misdiagnosed and mistreated each year[12,13,20].

Recent advancements in POC diagnostic tools, which specifically target developing country environments, have attempted to close this gap[14]. Nevertheless, despite advancements in increasing specificity, including RDTs that can identify the particular strain of malaria, little improvements have been made to increase the sensitivity of the detection method[17,18,19]. As WHO has made increased malaria surveillance one of its top priorities, being able to detect malaria in asymptomatic

individuals has emerged as an important goal[12,16,21]. One way to achieve this goal is to decrease the number of parasites/μL needed to detect malaria to levels that correspond with early stage malaria infection[12,21].

Red Blood Cell Deformability

RBCs can be considered elastic bodies since they must significantly deform as they pass through capillaries[3]. However, the mechanical properties of RBCs drastically change during malaria infection, which causes increased membrane rigidity and decreased deformation[6,8,9]. Principally, it has been found that cell deformability plays a major role in the pathogenesis of malaria because, at the onset of malaria infection, the parasitic inclusion and maturation processes cause cellular and molecular changes, drastically reducing RBC deformability[3,8]. Specifically, based on the stage of parasite maturation in the erythrocyte, *i*RBCs range from 3-50 times more stiff than healthy RBCs[8]. In addition to increased stiffness due to the inclusion of the parasite, the infected RBC (*i*RBC) can also be stiffened though the presence of crosslink actin in the cytoskeleton[9]. Thus, since RBC deformability has important implications for disease pathology, this knowledge can be exploited to better understand and diagnose malaria infections[1,2,3,45,8,9]. Relevant to this study, it has been determined that this variance in cell stiffness is significant at a microscopic scale and can be differentiated[8,10]. Quantifying this difference in RBC deformability during a malaria infection could allow for earlier diagnosis of malaria via enrichment of *i*RBCs from healthy RBCs.

Bow (2011) discusses commonly used methods to study RBC deformation including filtration and laser diffraction ellipsometry. However, these methods are not useful in clinical situations since the number of *i*RBCs will be small compared to the

larger population of healthy RBCs. Thus, other methods such as Atomic Force Microscopy (AFM), optical stretching, and optical tweezers should be used. Although Bow (2011) discusses several of these methods for examining RBC and *i*RBC elasticity, he ultimately choses to design a microfabricated device similar to a single micropipette aspirator. Although Bow certainly avoids treating the RBCs as a static system by developing his own device, his results were not significantly different from other methods that are easier and less time intensive to quantify baseline RBC deformability. Thus, he does not make a cogent argument against using simpler methods to quantify stiffness and deformability. As a result, AFM will be used in this study to determine RBC deformation.

Moreover, Eaton (2011) notes that the initial hepatocyte (liver cell) infection by the *Plasmodium* parasite is a clinically silent, obligatory step of the parasite's life cycle. Since hepatocyte infection occurs before RBC parasitic infection, Eaton hypothesizes that demonstrating that malaria infected liver cells also exhibit a change in deformability similar to that of *i*RBCs (Eaton 2011) could allow for the development of microfluidic diagnostic tools with the ability to diagnose malaria even earlier than the initial RBC infection stage. Whether liver stage diagnosis of malaria is clinically possible or necessary remains unknown. Given the limited time between infection of liver cells and RBCs, it is possible that focusing on changes in RBC deformability to diagnose malaria, instead of focusing on changes in hepatocyte deformability, will be just as clinically relevant and important for early malaria diagnosis. Moreover, it is clinically

simpler to obtain a blood sample than a hepatocyte sample from an infected individual in a rural, developing setting.

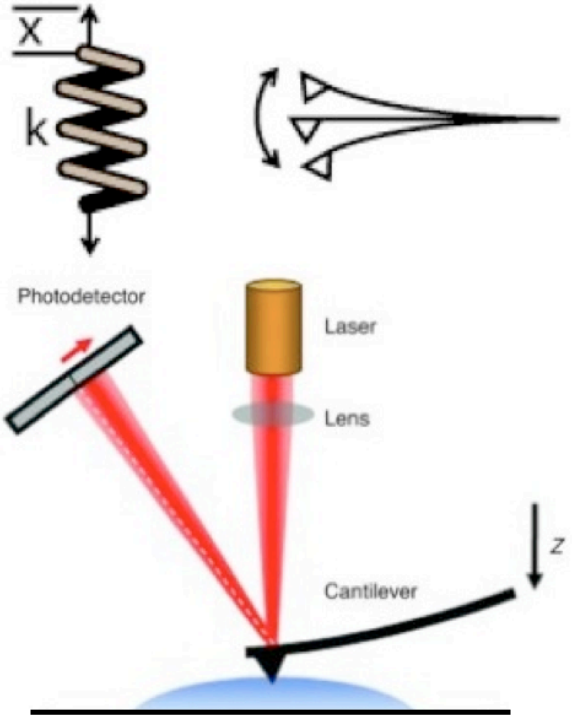

Figure 5. Atomic Force Microscopy General Overview

Atomic Force Microscopy

Atomic Force Microscopy (AFM) is a highly sensitive tool for measuring cell deformation or stiffness (force spectroscopy). Young's Modulus is calculated as a mechanical probe, or cantilever, indents into a cell and the resulting piezoelectric displacement is measured using the reflection of a laser into an array of photodiodes (**Figure 5**). This extension and retraction of the cantilever is recorded onto a force versus indentation graph. The slope of the curve after the cantilever makes contact with the cell is then used to determine Young's Modulus through a Hertz contact model.

Ebner's paper (2011) discusses the use of Atomic Force Microscopy (AFM) with regards to determining cell deformability. Specifically, he discusses the different AFM techniques that can be used to investigate healthy and pathological RBCs. This study set a precedent for ensuring the immobilization of whole, intact RBCs for analysis as it reported the importance of maintaining cell viability and proper cell culture conditions when conducting AFM measurements in order to better mimic normal, healthy cell environments. It has been shown that extensive changes in temperature, pH, and media content can alter cell stiffness. Thus, Ebner clearly demonstrates the need to limit

environmental changes such that a static model (AFM) can be applied to a dynamic system (RBC in body).

Microfluidic Platforms

The majority of research teams currently developing deformability-based diagnostic tools are using microfluidic platforms. Microfluidic devices precisely manipulate geometrically contained fluids for separation at the micrometer scale. In particular, it has been found that when using deformability as the separation factor, continuous-flow microfluidics are easier to implement and more sensitive than protein-sensing alternatives[1,4,5]. While microfluidic platforms were originally developed for use within the field of cancer diagnostics, given that it was one of the first diseases with a quantified difference in elastic modulus between healthy and malignant cells, the technology has since been applied to other diseases given increased knowledge of the changes in cellular mechanics other diseases.

Gascoyne (2004) and his research assistants were the first research team to recognize the ability to apply microfluidic technology to malaria detection. In particular, his research team compared the advantages and disadvantages of current malaria detection methods and discussed their adaptability towards integration with new microfluidic devices. Nevertheless, although Gascoyne extensively discussed challenges associated with developing better systems for detection, he did not discuss any methods to overcome these challenges and produce a viable option for malaria diagnosis/detection. Regardless, he concluded that, due to the potential benefits of microfluidic devices, the approach is worth pursuing.

Since 2004, there have been vast improvements in this research area, and, starting in 2010, the application of microfluidics to RBC deformability-based separation has become much more mainstream. Sha Huang and Han Wei Hou direct two prominent research groups working on this topic.

Huang (2010) looks at the difference in stiffness of healthy RBCs and *i*RBCs in microfluidic devices as a function of temperature. Specifically, he found that while *i*RBCs are less deformable than healthy RBCs at all temperatures, this difference in stiffness is maximized at 40 degrees celcius. Understanding this change in stiffness, perhaps due to the presence of a fever when infected with Malaria, is important to understanding how the malaria *Plasmodium* parasite alters the cell mechanics. Furthermore, Huang indicates that using warmer RBCs in microfluidic "deformability cytometry" could lead to improved malaria microfluidic diagnostics due to the larger statistical difference in stiffness.

Han Wei Hou has produced several papers on the application of microfluidic platforms for malaria detection over the past two years. In 2011, he reported several issues to be considered when designing a microfluidic, POC device for malaria detection. Specifically, he highlighted the importance of initial blood separation in order to enrich a certain aspect of the blood. This method is important since by separating healthy RBCs and *i*RBCs, it is possible that malaria could be detected earlier by using the aggrate to enrich the changes in stiffness found in the *i*RBC population. Enriching the *i*RBC population is crucial for the study's aim to improve the sensitivity of the current malaria RDT since it could allow for detection of malaria at levels around 10 parasites/μL (1/20 of the current sensitivity). Moreover, in 2012, Hou specifically addresses the issue of

platlet and White Blood Cell (WBC) filtration from whole blood. When looking for pathogen removal of a system, or pathogen separation for diagnostics, it is important to isolate the pathogen or marker cell. Thus, having some sort of filtration system prior to Red Blood Cell (RBC) separation will greatly aid in a POC malaria diagnostic, microfludic tool since whole blood can be used.

CHAPTER 2

METHODOLOGY

Red Blood Cell Preparation

Reagents

Citrate-dextrose solution (ACD), Poly-L-lysine (PLL), diamide (DIA), formaldehyde (FMA), and glutaraldehyde (GLA) were obtained from Sigma-Aldrich. Dulbecco's Phosphate Buffered Saline (DPBS) was obtained from Invitrogen.

Cell Culture

Whole blood was obtained by venipuncture from normal healthy donors of various blood types and treated immediately with 0.5% (by volume) ACD to prevent clotting. Blood was stored at 37°C until use. All experiments were conducted within 2 hours of the initial blood donation to prevent any inhibiting effects from using old blood.

RBC Isolation

RBCs were isolated (**Figure 6**) from whole blood through centrifugation at 1000 RCF for 10 minutes. The isolated RBCs were subsequently washed twice with DPBS. RBCs were diluted to a concentration of 1 million/mL for treatment with the various drugs that mimic the stiffening pathophysiology of malaria iRBCs. RBCs were diluted to a concentration of 50 million RBCs/mL for separation experiments and to a concentration of 3,000 RBCs/mL for AFM experiments. All RBC solutions were diluted in DPBS.

RBC Preparation

Four experimental groups were used: normal healthy RBCs and three different chemically mimicked *i*RBCs. The chemically treated RBCs mimicked the stiffening pathophysiology during malaria infection. Healthy RBCs were defined as the normal, untreated RBC population. Chemically micked *i*RBCs were created through treatment with (1) 4% FMA for 30 minutes at room temperature, (2) 4% GLA for 30 minutes at room temperature, and (3) 40 μM DIA for 20 minutes on ice. After treatment, the chemically mimicked *i*RBCs were subsequently washed twice with DPBS.

Figure 6. Red Blood Cell Isolation

Atomic Force Microscopy

Atomic Force Microscopy (AFM) was used to determine the deformability of RBCs. All RBCs were measured in a suspended state. Following RBC isolation, 3,000 RBCs were removed from each sample to create a cell suspension in 3 mL DPBS as shown in **Figure 7**. Glass AFM

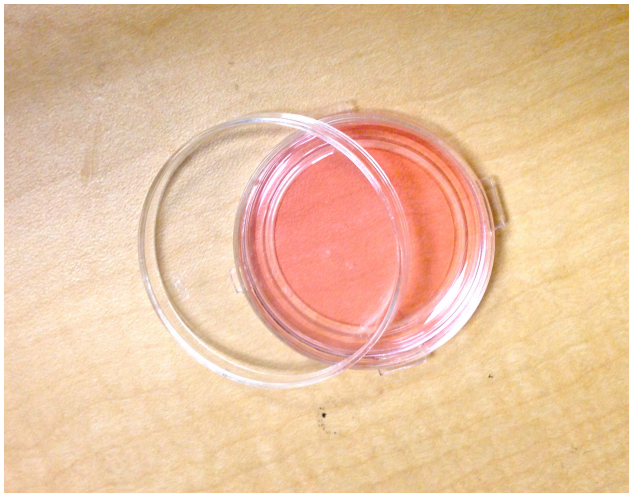

Figure 7. Red Blood Cell Suspension in AFM Fluorodish

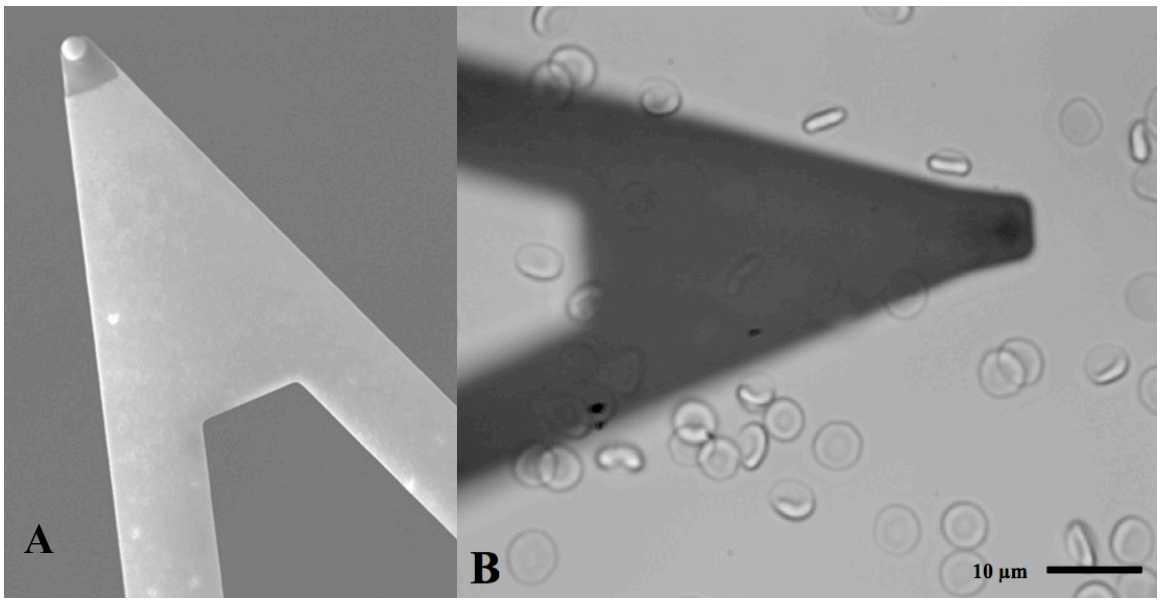

Figure 8. MSCT Triangular Silicon-Nitride Cantilever. A) Cantilever was beaded with a 5µm silica bead B) Cantilever during RBC elasticity measurements

fluorodishes (World Precision Instruments) were treated with 0.01% PLL prior to the addition of the RBC solution for enhanced cell plating. The monolayer of PLL on the fluorodish enhanced the ability to take AFM measurements by lightly attaching the cells to the glass without altering RBC morphology. Deformability measurements were collected using a MFP-3D AFM (Asylum Research) attached to an inverted optical microscope (Nikon Eclipse Ti) and a triangular, silicon nitride MSCT cantilever (Bruker). The cantilever (**Figure 8**) was calibrated using a thermal vibration method to determine the spring constant (0.03 N/m) and was positioned above the center of a single RBC prior to indentation. Individual RBCs (n=25) were indented 0.1 µm by the cantilever. Three force-indentation curves were generated for each measured RBC; the slope of each curve was then analyzed using a Hertz contact model for a pyramidal tip to obtain the cell's Young's Modulus.

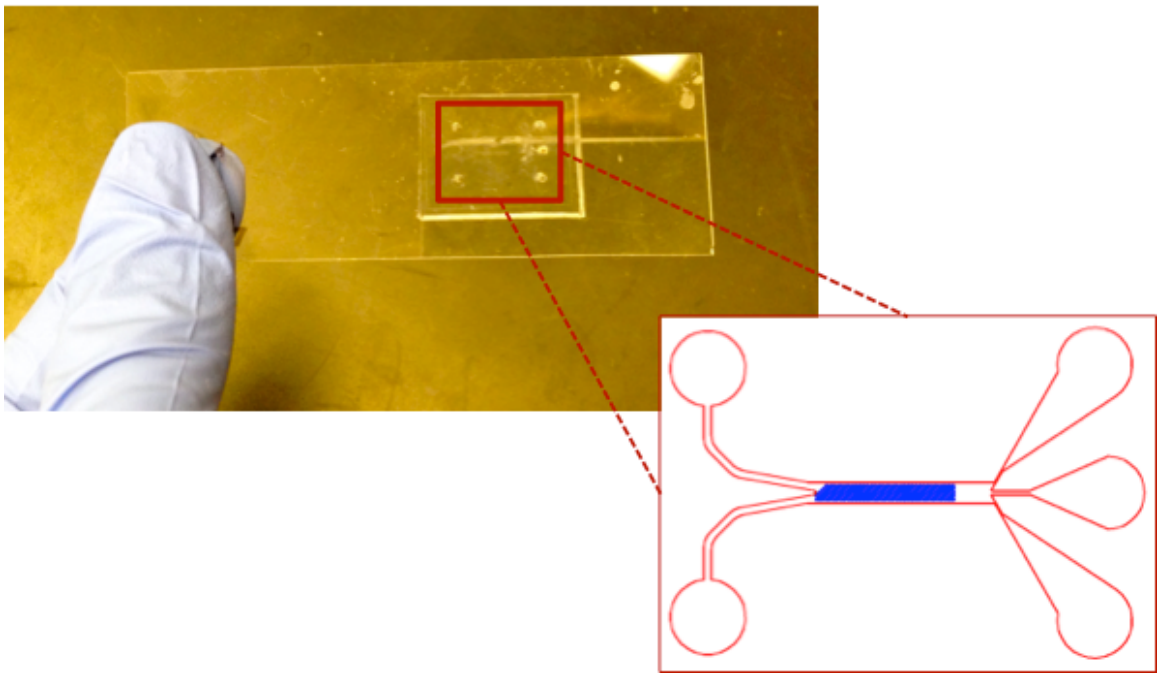

Figure 9. Microfluidic Device (Life Size). Image shows the high-throughput microfluidic device used for the stiffness-dependent separation of RBCs for early malaria detection.

Separation Experiments

Microfluidic devices (**Figure 9**) were designed and fabricated as previously described[21]. The microfluidic platform was developed based on a separation principle in which cells flowing through the microchannel are deformed by the periodic ridges which are skew to the channel. This elastic deformation produces a resultant mechanical force along the direction of the ridges. Stiff cells experience greater ridge-induced force, resulting in a greater transverse displacement parallel to the diagonal ridges; soft cells experience little ridge-induced force, resulting in a smaller transverse displacement parallel to the diagonal ridges and thus the cells more closely follow the original fluid streamlines.

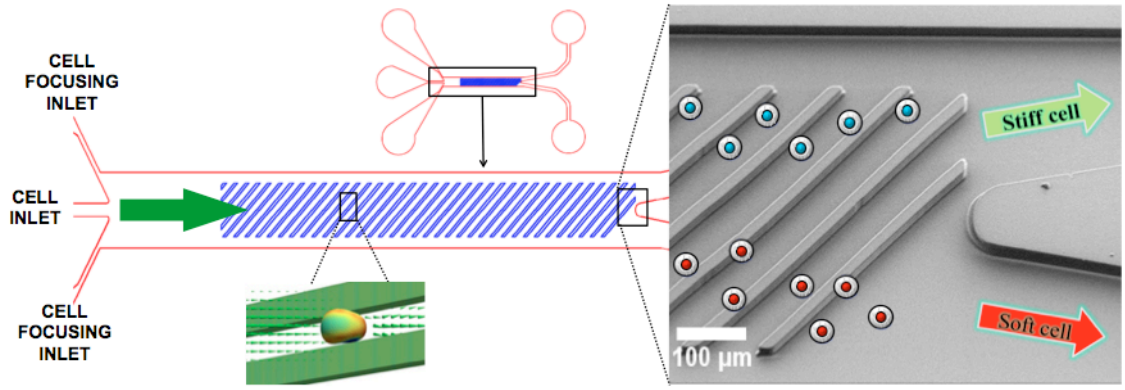

Figure 10. Microfluidic Device Concept Overview. Healthy and chemically stiffened RBCs were mixed prior to flowing. Using a microfluidic platform developed in conjunction with a computational Lattice Spring Model (LSM), cells were sorted by stiffness. Stiff cells (chemically mimicked iRBCs) were collected in the top outlet, while soft cells (healthy RBCs) were collected in the bottom outlet.

Biomechanical separation was tested using syringe pumps to control the flow rates of both the cell solution and cell focusing sheaths across the microchannels (**Figure 10**). Single flow separation experiments occured first; during these experiments, normal RBCs and chemically mimicked *i*RBCs were separated individually through microfludic devices with varying gap sizes at a range of flow rates. After identifying the ideal flow rate and gap size for the microfluidic technology, the specific cell trajectories, illstrating the amount and direction of transverse displacement, were calculated to illustrate the ability to separate the two otherwise identical populations. Once the ability to separate two populations was confirmed by comparing net transverse displacement per ridge, combined solutions of both RBC and *i*RBCs populations were separated.

Red Blood Cell Size Determination

To ensure that we were separating populations that only varied by elasticity, not size, all tested RBC populations were imaged and the average diameter was measured.

CHAPTER 3

RESULTS

Red Blood Cell Size

RBCs were imaged using phase contrast microscopy at 40x. Images were then processed via ImageJ software to determine the average RBC diameter of each treatment group (healthy, DIA-treated, FMA-treated, and GTA-treated RBCs). It was determined that there was no statistical difference ($p>0.05$) in cell size between the four groups. In particular, healthy RBCs had an average diameter of 8.82 ± 0.50 µm, DIA-treated RBCs had an average diameter of 8.63 ± 0.62 µm, FMA-treated RBCs had an average diameter of 8.64 ± 0.64 µm, and GTA-treated RBCs had an average diameter of 8.73 ± 0.62 µm. Representative images of these cell populations can be found in Figure 12.

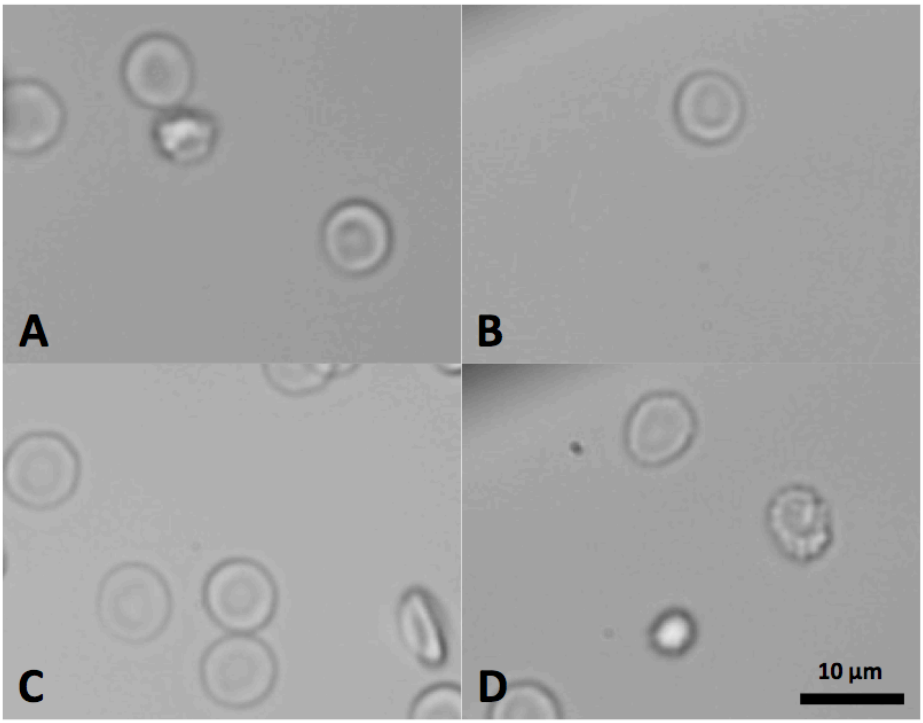

Figure 11. Representative Images of Red Blood Cell Morphology and Size. A) DIA-treated RBCs B) FMA-treated RBCs C) healthy RBCs D) GTA-treated RBCs. No statistical differences were found in cell size between any of the tested groups, confirming that each group only differs in cell elasticity. Thus, cells are being separated by elasticity, not by some other factor such as size.

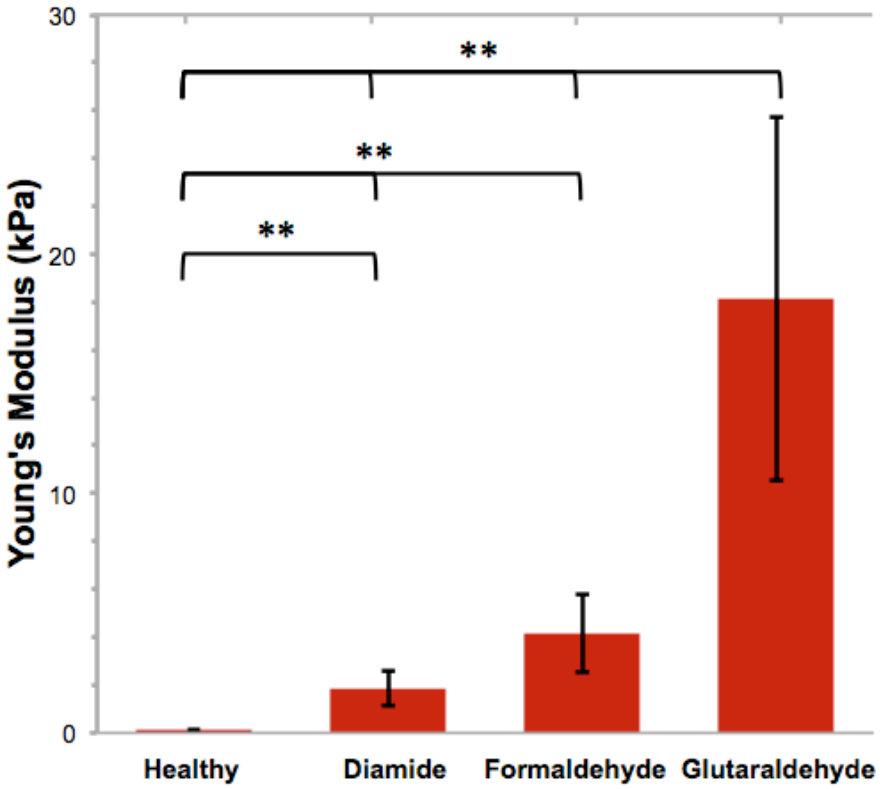

Figure 12. Deformability Results of Red Blood Cells. RBCs were treated with various drugs (DIA, FMA, and GTA) to simulate the stiffening pathophysiology during a malaria infection. Young's Modulus was measured using Atomic Force Microscopy in conjunction with a Hertz contact model.

Red Blood Cell Young's Modulus

Atomic Force Microscopy (AFM) was used to calculate the Young's Modulus of healthy RBCs and chemically mimicked *i*RBCs. Baseline elasticity measurements (**Figure 12**) for healthy RBCs and chemically stiffened RBCs (n=25) showed a significant statistical difference ($p<0.001$) between all tested groups. In particular, healthy RBCs (E= 0.102 ± 0.043 kPa) were found to be statistically more deformable than DIA-treated RBCs (E= 1.867 ± 0.728 kPa), FMA-treated RBCs (E= 4.267 ± 1.608 kPa), and GTA-treated RBCs (E= 18.513 ± 7.761 kPa) (**Table 1**). This further demonstrated that two of the selected drug treatments, DIA and FMA, could correctly mimic the stiffening pathophysiology of early *i*RBCs since they were found to have a

Young's Modulus within the desired literature range of 3-50 times less deformable than healthy RBCs[8].

Type of RBC	Young's Modulus	Comparison of Elasticity
Healthy RBCs	0.102 ± 0.043 kPa	---
DIA-treated RBCs	1.867 ± 0.728 kPa	18x
FMA-treated RBCs	4.267 ± 1.608 kPa	42x
GTA-treated RBCs	18.513 ± 7.761 kPa	185x

Table 1. Deformability of Red Blood Cells

Red Blood Cell Separation Experiments

Single flow experiments of only one experimental RBC population were conducted first to ascertain the correct parameters for separation, including flow rate and device dimensions, particularly the gap distance between the ridges and the bottom of the channel. Specifically, normal RBCs and chemically stiffened RBCs were separated individually through microfludic devices with varying gap sizes (2, 4, 6, and 8 μm) at a range of flow rates (0.0001, 0.0005, 0.001 mL/min). It was found that the healthy RBCs exited the device in the bottom inlet for all test cases; however, the three chemically stiffened populations experienced varied effects. The FMA-treated RBCs exited at the top outlet, typical of stiff cells, at gaps of 2 and 4 μm and with all flow rates of 0.0001 mL/min. The GTA-treated RBCs only exited at the top outlet at gaps of 2 and 4 μm and with flow rates of 0.0001 mL/min. The DIA-treated cells did not exhibit any downwards displacement at any of the tested gap size or flow rates. Thus, the device constaints for

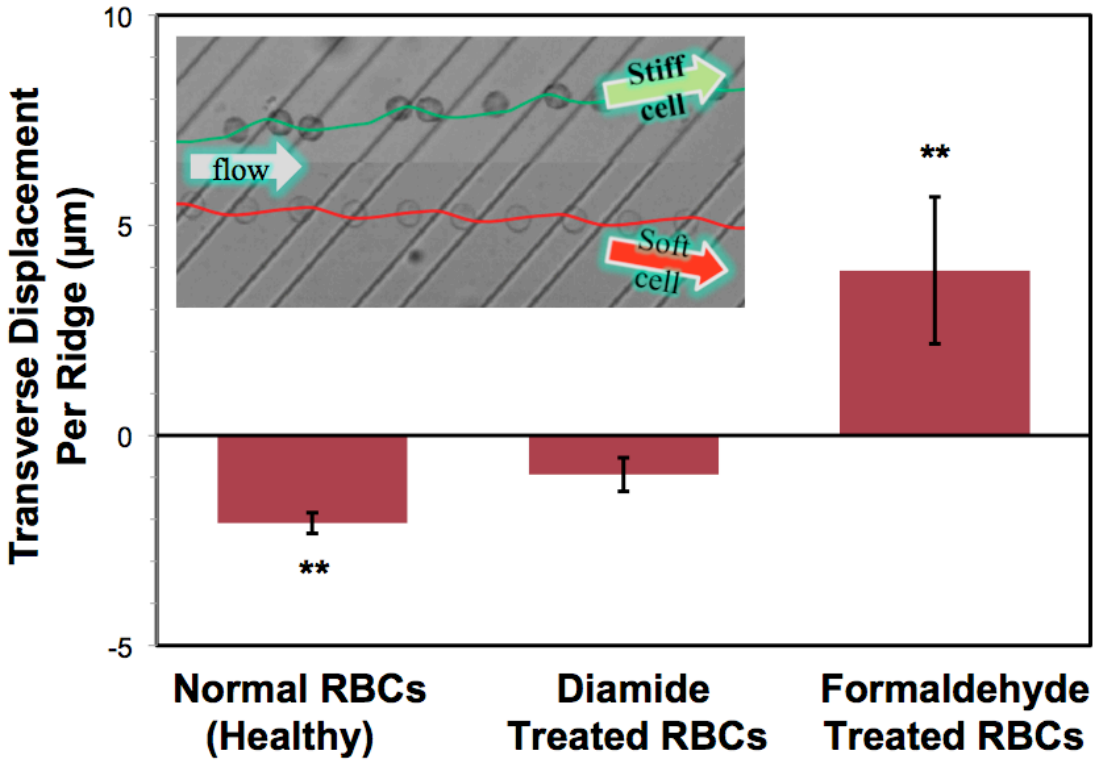

Figure 13. Single Flow Trajectory Results. The trajectories of single RBCs over the device's periodic ridges were analyzed by calculating the net transverse displacement per ridge. This displacement value and direction was then used to determine the ability to separate two RBC populations if combined.

separation were determined to be a device with gaps between ridges of 2-4 µm that used low flow rates of 0.0001 mL/min.

Using the results of flowing single populations of RBCs at this gap size and flow rate, the specific RBC trajectories over the periodic ridges were analyzed by calculating the net transverse displacement per ridge (**Figure 13**). Healthy RBCs had a net negative displacement of -2.08 µm, DIA-treated RBCs had a net negative displacement of -0.93 µm, and FMA-treated RBCs had a net positive displacement of 3.92 µm. These displacement results demonstrated the ability to separate healthy RBCs and FMA-treated RBCs given that healthy RBCs experienced negative displacement while FMA-treated RBCs experienced positive displacement. Thus, subsequent separation experiments

(**Figure 14**) were conducted using combined solutions of both RBC and *i*RBCs populations with a 4 μm device and a 0.0001 mL/min inlet flow rate. However, despite theoretical confirmation of the ability to biomechanically separate the two populations, preliminary visual results have not exhibited the expected outcome: it could not be quantitatively determined that the two populations separated from each other via the microfluidic platform.

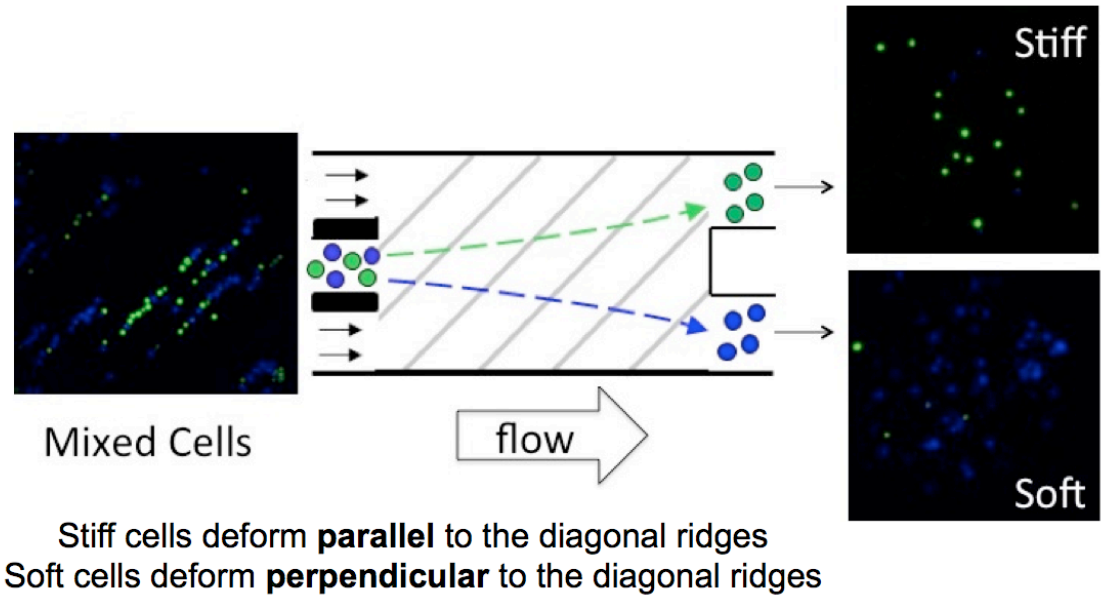

Figure 14. Combined Solution Separation Experiment Overview. Healthy RBCs and FMA-treated RBCs were combined and flowed through the microfluidic platform. It was expected that the stiff cells (mimicked *i*RBCs) would have a net positive displacement and be collected in the top outlet, while the soft cells (healthy RBCs) would have a net negative displacement e collected in the bottom outlet. However, this was not immediately observed. Thus, additional testing must occur.

CHAPTER 4

DISCUSSION

Red Blood Cell Deformability

Given this significant difference in RBC elasticity among all groups ($p<0.001$), and the fact that the chemically treated RBCs ranged from 3-50 times less deformable than the healthy RBCs, it was determined that two of the selected drug treatments (FMA and DIA) could correctly mimic the stiffening pathophysiology of *i*RBCs. In particular, the various stages of a malaria infection can be indicated via differences in RBC deformability: as the parasite matures in the RBC and/or the parasitemia of the blood increases, the difference in stiffness between *i*RBCs and RBCs also increases. Thus, the statistical difference ($p<0.01$) between mimicked *i*RBC treatment groups illustrated that there were four distinct populations. Given that the three treated RBC populations had Young's Moduli that ranged from 3-50 times less deformable than the healthy RBC population, it was determined that the three experimental groups could simulate various stages of the stiffening pathophysiology of *i*RBCs. Furthermore, given this significant nanomechanical difference in elasticity among all groups, it was determined that the four RBC populations could be differentiated on a microscopic scale using stiffness-based microfluidic separation.

Red Blood Cell Separation

The single flow experiments confirmed the ability of the proposed microfluidic device to separate otherwise identical populations of RBCs that only varied by stiffness.

Particularly, this was confirmed by tracking the different RBC trajectories through the microfluidic device from inlet to outlet and calculating the net transverse displacement of the various RBC populations (Healthy, DIA, FMA, and GTA). Healthy RBCs had a net negative displacement of -2.08 μm, DIA-treated RBCs had a net negative displacement of -0.93 μm, and FMA-treated RBCs had a net positive displacement of 3.92 μm. These displacement results demonstrated the ability to separate healthy RBCs and FMA-treated RBCs given that healthy RBCs experienced negative displacement while FMA-treated RBCs experienced positive displacement.

Furthermore, the displacement results were used to ascertain the theoretical ability to separate two experimental populations (Healthy vs. DIA, FMA or GTA) that only varied in elasticity by using a microfluidic platform. Given theoretical confirmation of the ability to biomechanically separate healthy and FMA-treated RBCs, preliminary separation experiments of combined solutions were conducted. Regardless, preliminary visual results did not exhibit the expected theoretical outcome: it was not quantitatively determined that the two populations could be separated from each other using highthroughput biomechanical separation. This inability to quantiatively demonstrate separation of identical populations of RBCs that only varied by stiffness (E= 0.102 kPa and E= 4.267 kPa) at a throughput of 200 million cells/min could be due to several confounding factors. First, given that RBCs are not perfect spheres, their ridge-induced translation might not respond as predicted by computational simulations. In additional, due to the high flow rates, the dynamic stiffness may be different than the values determined with AFM. Moreover, it is possible that the device's dimensions were not fully optimized for this non-spherical RBC shape; separation could occur by further

adjusting the gap height. Finally, the RBC stains were not optimized as we observed co-staining of both cell populations after separation occurred. We anticipate that improvements in cell staining and more exact device parameters will lead to significantly improved RBC enrichment.

CHAPTER 5

CONCLUSIONS

Red Blood Cell Deformability

It was found that there exists a significant difference in elasticity between healthy RBCs and chemically mimicked *i*RBCs (RBCs treated with DIA, FMA or GTA). This significant elasticity variance mimics the natural change in cellular mechanical properties during a malaria infection, which causes increased RBC membrane rigidity and decreased deformation. It was shown that this variance is significant at a microscopic scale and can be exploited for diagnostic purposes via stiffness-dependent cell separation resulting in population differentiation and enrichment of the number of parasites per milliliter.

Red Blood Cell Separation Experiments

It was determined that a microfluidic platform that separates cells by mechanical stiffness can be successfully employed. Particularly, it was shown that the periodic ridges of the microfludic device deform RBCs and that this elastic deformation allows for stiffness-dependent separation by producing mechanical forces along the ridges that act on soft and stiff cells differently: stiff cells experience this ridge-induced force, resulting in transverse displacement parallel to the diagonal ridges, while soft cells experience little ridge-induced force, resulting in transverse displacement perpendicular to the diagonal ridges. Thus, it was determined that the separation of healthy and FMA-treated RBCs, which mimic early stage *i*RBCs, can occur. This result was used to initiate preliminary separation experiments of two combined RBC populations: healthy RBCs and FMA-

treated RBCs. However, combined separation experiments of healthy RBCs and FMA-treated RBCs did not yield the expected theoretical separation/enrichment results. Rather, it was visually determined in all trials that separation did not occur. Thus, several future changes must occur in order to ensure the experimental combined RBC separation results match the experimental single flow RBC results. These changes are discussed in the the subsequent section.

CHAPTER 6

FUTURE WORK

Combined Solution Separation Experiments

Given initial that preliminary combined separation experiments did not exhibit the expected separation outcome, future studies will specifically address potential counfounding factors or barriers to the combined separation of healthy RBCs and FMA-treated RBCs. For example, since RBCs are not perfect spheres, their ridge-induced translation might not respond as predicted by computational simulations. In additional, due to the high flow rates, the dynamic stiffness may be different than the values determined with AFM. Moreover, it is possible that the device's dimensions were not fully optimized for this non-spherical RBC shape; thus, separation could occur by further adjusting the gap height, not just the gap width. Finally, since the results of the combined separation experiments were visually determined and we observed co-staining of both cell populations after separation occurred, future studies will utilize optimized RBC stains to quantitatively determine percent population both prior and post separation. Thus, we anticipate that improvements in cell staining and more exact device parameters will lead to significantly improved RBC enrichment. These future results will enable the future development of microfluidic technologies for malaria diagnosis and population surveillance that improve on the sensitivity of the current Rapid Diagnostic Test (RDT). If successful separating mimicked *i*RBC separation from healthy RBCs, subsequent stages of this study will transition to separating malaria blood samples, which contain both healthy RBCs and actual malaria *i*RBCs.

Whole Blood Separation Experiments

If successful with combined solution separation, future studies will also transition to whole blood separation to better mimic potential point-of-care field use for malaria detection. Currently, RBCs are isolated from whole blood and diluted x50 to ensure that the device does not clog. However, the isolation and dilution of RBCs requires both training and laboratory equipment. Thus, it is not always possible or desired in endemic, developing areas. It is crucial that this step either be minimized or removed to better facilitate ease-of-use and, as a result, increase the liklihood that the device will be used to diagnose and enhance surveillance of malaria in neglected areas. In order to achieve this, additional alterations to the exisiting device must be considered. For example, a preliminary while blood cell filter must be added to isolate RBCs from the whole blood population prior to separation via the diagnoal ridges.

APPENDIX A

SINGLE FLOW RBC TRAJECTORY VIDEO

This file demonstrates the trajectory of healthy RBCs flowing through the described microfluidic platform.

APPENDIX B

RBC SEPARATION VIDEO

This file illustrates the two trajectories of a combined solution of healthy RBCs and FMA-treated RBCs during separation via a stiffness-dependent microfluidic platform.

REFERENCES

1. Gascoyne, P. *Microfluidic Approaches to Malaria Detection*. Acta Tropica 89(3): 357-369. 2004.

2. Zhang, R. *Application of Microfluidic Device to Malaria Diagnosis*. Massachusetts Institute of Technology: 45-47. 2007.

3. Bow, H. *A Microfabricated Deformability-Based Flow Cytometer with Application to Malaria*. The Royal Society of Chemistry 11: 1065-1073. 2011.

4. Huang, S. *Applying a Microfluidic 'Deformability Cytometry' to Measure Stiffness of Malaria-Infected Red Blood Cells at Body and Febrile Temperatures.* Miniaturized Systems for Chemistry and Life Sciences 14: 256-261. 2010.

5. Hou, HW. *A Microfluidics Approach Towards High-Throughput Pathogen Removal from Blood Using Margination.* American Institute of Physics: Biomicrofluidics 6(024115): 1-13. 2012.

6. Eaton, P. *Infection by Plasmodium Changes Shape and Stiffness of Hepatic Cells.* Nanomedicine: Nanotechnology, Biology, and Medicine 8: 17-19. 2011.

7. Ebner, A. Normal and Pathological Erythrocytes Studied by Atomic Force Microscopy. Methods in Molecular Biology 736: 223-241. 2011.

8. Dondorp, AM. *Red cell deformability as a prognostic factor in severe falciparum malaria.* American Journal of Tropical Medicine and Hygiene. 57: 507-511. 1997.

9. Hou, HW. *Deformability Based Cell Margination for Malarial Infected Red Blood Cell Enrichment.* Miniaturized Systems for Chemistry and Life Sciences 14: 1370-1372. 2010.

10. Fuhrmann, A. *AFM Stiffness Nanotomography of Normal, Metaplastic, and Dysplastic Human Esophageal Cells.* Physical Biology 8(1): 1-10. 2011.

11. Centers for Disease Control and Prevention. *Malaria*. http://www.cdc.gov/malaria/. Accessed August 2013.

12. World Health Organization. *Universal Access to malaria diagnostic testing- An operational manual*. World Health Organization Manuals. 2011.

13. Guerin, P. *Malaria: current status of control, diagnosis, treatment, and a proposed agenda for research and development*. The Lancet Infectious Diseases. 2(9):564-573. 2002.

14. Breman, J. *Conquering Malaria (Chapter 21).* Disease Control Priorities in Developing Countries. 2nd edition. 2006.

15. Tangpukdee, N. *Malaria Diagnosis: A Brief Review*. Korean Journal of Parasitology. 47(2): 93-102. 2009.

16. World Health Organization. *Malaria Surveillance*. http://www.who.int/malaria/areas/surveillance/en/. Accessed August 2013.

17. Bell, D. Ensuring quality and access for malaria diagnosis: how can it be achieved?. Nature Reviews Microbiology. 4(9): 682-695. 2006.

18. Greenwood, BM. Malaria: progress, perils, and prospects for eradication. Journal of Clinical Investigation. 118(4): 1266-1276. 2008.

19. Moody, A. Rapid diagnostic tests for malaria parasites. Clinical Microbiology Reviews. 15(1): 66. 2002.

20. Amexo, M. *Malaria misdiagnosis: effects on the poor and vulnerable.* The Lancet. 364(9448): 1896-1898. 2004.

21. Sturrock, H. *Targeting Asymptomatic Malaria Infections: Active Surveillance in Control and Elimination*. PLoS Medicine. 10(6): e1001467. 2013.

22. Wang, G. *Stiffness Dependent Separation of Cells in a Microfluidic Device.* PLoS ONE. 8(10): e75901. 2013.

23. Malaria Vaccine Initiative. *Life Cycle of the Malaria Parasite.* MVI/PATH. Accessed August 2013. http://www.malariavaccine.org/malvac-lifecycle.php

VITA

REBECCA BYLER

BYLER was born in Denver, Colorado. She attended elementary, middle, and high school in Palo Alto, California before moving to Georgia for college. She will receive a B.S. in Biomedical Engineering with minors in Chemistry, Women's Studies, and Spanish from Georgia Institute of Technology in December 2013. After taking a gap year to backpack Antarctica and South America, Ms. Byler will begin her graduate studies at Yale University in August 2014. When she is not working on her research, Ms. Byler enjoys playing soccer, baking desserts, and volunteering in Atlanta.